



# Prognosis after Curative Resection of Single Hepatocellular Carcinoma with A Focus on LI-RADS Targetoid Appearance on Preoperative Gadoteric Acid-Enhanced MRI

Ji Yoon Moon<sup>1</sup>, Ji Hye Min<sup>2</sup>, Young Kon Kim<sup>2</sup>, Donglk Cha<sup>2</sup>, Jeong Ah Hwang<sup>2</sup>, Seong Eun Ko<sup>2</sup>, Seo-Youn Choi<sup>3</sup>, Eun Joo Yun<sup>1</sup>, Seon Woo Kim<sup>4</sup>, Ho-Jeong Won<sup>4</sup>

<sup>1</sup>Department of Radiology, Kangdong Sacred Heart Hospital, Hallym University College of Medicine, Seoul, Korea; <sup>2</sup>Department of Radiology and Center for Imaging Science, Samsung Medical Center, Sungkyunkwan University School of Medicine, Seoul, Korea; <sup>3</sup>Department of Radiology, Soonchunhyang University College of Medicine, Bucheon Hospital, Bucheon, Korea; <sup>4</sup>Biostatistics and Clinical Epidemiology Center, Research Institute for Future Medicine, Samsung Medical Center, Seoul, Korea

**Objective:** To evaluate the prognostic implications of preoperative magnetic resonance imaging (MRI) features of hepatocellular carcinoma (HCC) with a focus on those with targetoid appearance based on the Liver Imaging Reporting and Data System (LI-RADS), as well as known microvascular invasion (MVI) features.

**Materials and Methods:** This retrospective study included 242 patients (190 male; mean age, 57.1 years) who underwent surgical resection of a single HCC ( $\leq 5$  cm) as well as preoperative gadoteric acid-enhanced MRI between January 2012 and March 2015. LI-RADS category was assigned, and the LR-M category was further classified into two groups according to rim arterial-phase hyperenhancement (APHE). The imaging features associated with MVI were also assessed. The overall survival (OS), recurrence-free survival (RFS), and their associated factors were evaluated.

**Results:** Among the 242 HCCs, 190 (78.5%), 25 (10.3%), and 27 (11.2%) were classified as LR-4/5, LR-M with rim APHE, and LR-M without rim APHE, respectively. LR-M with rim APHE (vs. LR-4/5; hazard ratio [HR] for OS, 5.48 [ $p = 0.002$ ]; HR for RFS, 2.09 [ $p = 0.042$ ]) and tumor size (per cm increase; HR for OS, 6.04 [ $p = 0.009$ ]; HR for RFS, 1.77 [ $p = 0.014$ ]) but not MVI imaging features ( $p > 0.05$ ) were independent factors associated with OS and RFS. Compared to the 5-year OS and RFS rates in the LR-4/5 group (93.9% and 66.8%, respectively), the LR-M with rim APHE group had significantly lower rates (68.0% and 45.8%, respectively, both  $p < 0.05$ ), while the LR-M without rim APHE group did not significantly differ in the survival rates (91.3% and 80.2%, respectively, both  $p > 0.05$ ).

**Conclusion:** Further classification of LR-M according to the presence of rim APHE may help predict the postoperative prognosis of patients with a single HCC.

**Keywords:** Hepatocellular carcinoma; Diagnostic imaging; Liver; Magnetic resonance imaging; Prognosis

## INTRODUCTION

Hepatic resection is a curative treatment option for single hepatocellular carcinoma (HCC) in patients with well-preserved liver function [1-3]. However, surgical outcomes

remain unsatisfactory, with 5-year recurrence rates after hepatic resection up to 50–70% [4-6]. Presurgical identification of patients at high risk for tumor recurrence is important to help surgeons select surgical candidates and appropriate treatment options, including more aggressive

**Received:** December 6, 2020 **Revised:** April 18, 2021 **Accepted:** April 27, 2021

**Corresponding author:** Ji Hye Min, MD, PhD, Department of Radiology and Center for Imaging Science, Samsung Medical Center, Sungkyunkwan University School of Medicine, 81 Irwon-ro, Gangnam-gu, Seoul 06351, Korea.

• E-mail: minjh1123@gmail.com

This is an Open Access article distributed under the terms of the Creative Commons Attribution Non-Commercial License (<https://creativecommons.org/licenses/by-nc/4.0>) which permits unrestricted non-commercial use, distribution, and reproduction in any medium, provided the original work is properly cited.

surgery (anatomic rather than non-anatomic resection, wide resection margins), adjuvant clinical trials, or transcatheter arterial chemoembolization [7,8]. Therefore, the risk factors after hepatic resection have been extensively studied [7,9-11] and several imaging features have been reported to be associated with the prognosis of HCC [10,12-14].

The Liver Imaging Reporting and Data System (LI-RADS) was developed to facilitate a standardized imaging-based diagnosis of HCC [15]. Recent studies have suggested that LI-RADS categories are associated with the postoperative prognosis of primary liver cancer, independent of the pathologic diagnosis [16-18]. Rim arterial-phase hyperenhancement (APHE), a component of the LR-M (probably malignant, not specific for HCC) features, is also reportedly associated with poor HCC prognosis [10,18,19] as it is associated with aggressive histopathological features, including a more hypoxic and fibrotic tumor microenvironment. Thus, we hypothesized that the presence of rim APHE, among LR-M targetoid features, may play an important role in predicting the prognosis of HCC.

Among the various prognostic factors for HCC, microvascular invasion (MVI) is a well-known prognostic factor for HCC after surgical resection or liver transplantation [20]. Although MVI of HCC is a pathologically determined tumor factor, studies have attempted to identify imaging features for predicting MVI [21,22]. Among these, tumor size [22], tumor margin [21,23], rim APHE [14], peritumoral arterial enhancement [21,24], and peritumoral hypointensity in the hepatobiliary phase (HBP) of gadoxetic acid-enhanced magnetic resonance imaging (MRI) [11,21] have been proposed as predictors of MVI in HCC. However, there remains controversy, and the generalization of imaging features for predicting MVI may be subjective. Therefore, there is an unmet need for a simple and standardized summary of observations that can correctly reflect aggressive tumor biology and encompass known prognostic factors. We assumed that the LI-RADS category focusing on targetoid appearance would be simple and clinically easy to apply for prognostic prediction and compared the usefulness of this method to that for known MVI imaging features. To our knowledge, no study has reported the combined use of LI-RADS category and known MVI imaging features to predict the postoperative prognosis of HCCs.

Thus, this study evaluated the prognostic implications of preoperative MRI features of HCC, with a focus on LI-RADS with a targetoid appearance along with known MVI imaging

features.

## MATERIALS AND METHODS

The Institutional Review Board approved this study and waived the requirement for informed consent (IRB No. 2020-04-032).

### Patients

We retrospectively searched our institution's surgicopathological database for cases between January 2012 and March 2015 to identify patients who met the following inclusion criteria: 1) liver cirrhosis from any cause or chronic hepatitis B, 2) surgically resected single HCC ( $\leq 5$  cm in maximal diameter), 3) preoperative gadoxetic acid-enhanced liver MRI performed within 2 months of surgery, 4) no history of HCC treatment, and 5) at least 6 months of postoperative follow-up. We excluded patients with observation categorized as LR-tumor in vein (TIV) (nodule with definite TIV). Finally, this study included a total of 242 patients with HCC (Fig. 1). Among these patients, 185 were previously reported in a study from our institution [25]. However, the previous study focused only on the comparison

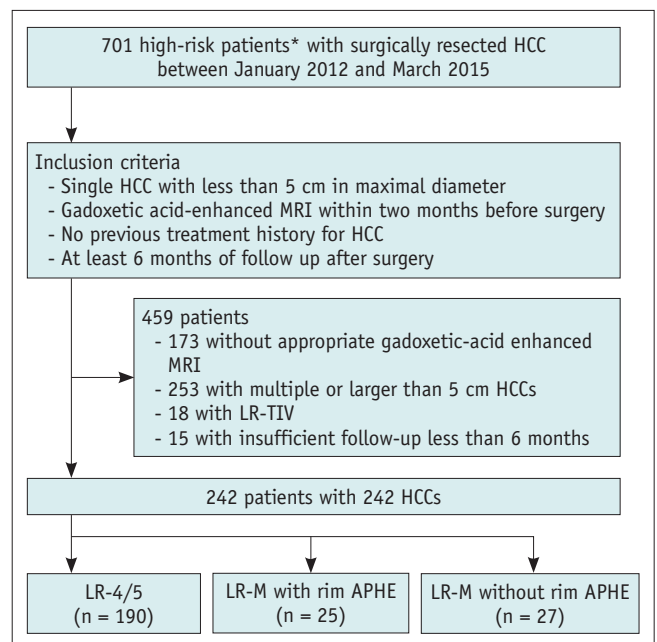


**Fig. 1. Flowchart of the study population.**

\*Liver cirrhosis of any cause or chronic hepatitis B. Liver Imaging Reporting and Data System categories were defined as LR-4 (probably HCC), LR-5 (definitely HCC), LR-M (probably malignant, not specific for HCC), and LR-TIV (nodule with definite tumor in vein). APHE = arterial-phase hyperenhancement, HCC = hepatocellular carcinoma, TIV = tumor in vein

of preoperative factors and both pre-/postoperative factors in the prediction of the early recurrence of HCC and did not consider LI-RADS categories. The current study evaluated the prognostic role of LI-RADS category after additional categorization of LR-M, as well as the known MRI features of MVI in HCC.

### Image Acquisition

MRI was performed using a 3Tesla MR system (Intera Achieva; Philips Healthcare). The routine protocol included T1-weighted, T2-weighted, and diffusion-weighted images at b-values of 0, 100, and 800 s/mm<sup>2</sup>. For dynamic contrast-enhanced imaging, T1-weighted three-dimensional turbo field-echo images were obtained before and after the intravenous administration of gadoteric acid (Primovist; Bayer Healthcare) using a power injector at 1–2 mL/s for a total dose of 0.025 mmol/kg body weight. The arterial phase (AP, 25–30 seconds), portal venous phase (60 seconds), transitional phase (TP, 3 minutes), and HBP (20 minutes) images were obtained; the AP timing was determined using an MR fluoroscopic bolus detection technique. The details are provided in Supplementary Table 1.

### Image Analysis

The image analysis was performed retrospectively by two abdominal radiologists (with 10 and 11 years of experience, respectively). The reviewers were aware of the presence of HCC but were blinded to the clinical, pathologic, and follow-up outcomes. They independently evaluated the presence of the following imaging features for each HCC: major features (size, non-rim APHE, non-peripheral washout, and enhancing capsule) and targetoid features (rim APHE, peripheral washout, delayed central enhancement, targetoid restriction, and targetoid appearance on TP or HBP images) based on LI-RADS v2018 [15]. Their observations were classified as category LR-4 (probably HCC), LR-5 (definitely HCC), or LR-M according to the major, ancillary, and LR-M features. The LR-M category was strictly assigned to nodules exhibiting any of the LR-M features. The LR-M group was further categorized as LR-M with and without rim APHE. Threshold growth was not evaluated because the analysis included only one examination per patient.

The reviewers also evaluated the following imaging features associated with MVI of HCC [21]: 1) non-smooth tumor margin, presenting as non-nodular tumors with a budding portion at the periphery [21,23]; 2) peritumoral enhancement on AP images, defined as a detectable portion

of a crescent- or polygonal-shaped enhancement outside the tumor margin with broad contact to the tumor border [21,24]; and 3) peritumoral hypointensity on HBP images, defined as a wedge-shaped or flame-like hypointense areas of hepatic parenchyma located outside the tumor margin [21,26].

After independent image review, the interobserver agreement was calculated. Discrepancies between the two reviewers were resolved by joint review with a third observer (with 20 years of experience in liver MRI) until a consensus was reached.

### Clinical-Pathologic Evaluation

The following characteristics were recorded from the patients' electronic medical records: the underlying cause of chronic liver disease, Child-Pugh grade, albumin-bilirubin (ALBI) grade, and serum alpha-fetoprotein (AFP) and protein induced by vitamin K absence or antagonist-II (PIVKA-II) levels within 2 months of hepatic resection. The histopathologic data of HCC, including tumor differentiation (Edmonson grade I, II, III, or IV) and MVI were acquired from the pathologic reports. MVI was defined as a tumor within a vascular space lined with endothelial cells that was visible by microscopy [27].

### Follow-Up after Surgical Resection

Routine postoperative surveillance at our institution consisted of physical examination and laboratory tests for AFP and PIVKA-II, with multiphasic abdominal CT or MRI performed every 1–3 months for the first 2 years and every 3–6 months thereafter. Overall survival (OS) and recurrence-free survival (RFS) were calculated as the time interval from surgery to death and the interval from surgery to tumor recurrence or death, respectively. After surgical resection, the patients were followed up until death or until the last follow-up date (May 31, 2019).

### Statistical Analysis

The baseline characteristics were analyzed using chi-squared or Fisher's exact tests (categorical variables) or Kruskal-Wallis tests with Wilcoxon rank-sum tests (continuous variables). Bonferroni corrections were used for pairwise comparisons between subgroups. Two-sided adjusted *p* values are reported. The Kaplan-Meier method and log-rank tests were used to evaluate the cumulative rates of HCC recurrence and death. Predictive factors for HCC recurrence and death were identified using a Cox

proportional hazard model. Variables with  $p < 0.1$  in univariable analysis were included in the multivariable regression analysis. Interobserver agreement for the presence of MRI features and LI-RADS category was evaluated using kappa ( $\kappa$ ) tests. The  $\kappa$  values were defined as follows: poor ( $< 0.20$ ), fair (0.21–0.40), moderate (0.41–0.60), good (0.61–0.80), and excellent (0.81–0.99) agreement.  $p < 0.05$  was considered statistically significant. Statistical analysis was performed using SAS version 9.4 (SAS Institute Inc.) and IBM SPSS Statistics for Windows, version 20.0 (IBM Corp.).

## RESULTS

### Patient Characteristics

The patient characteristics are summarized in Table 1. The study cohort consisted of 242 patients (mean age,  $57.1 \pm 9.8$  years [range, 31–84 years], including 190 male and 52 female). Chronic hepatitis B viral infection was the predominant cause of the underlying liver disease (82.2%, 199/242). A total of 108 (44.6%) patients had liver cirrhosis on histopathological specimens.

Among the 242 HCCs, 190 (78.5%) and 52 (21.5%)

were classified as LR-4/5 and LR-M, respectively. The LR-M category was reclassified into two groups according to the presence of rim APHE, with 25 (10.3%) HCCs classified as LR-M with rim APHE (Fig. 2) and 27 (11.2%) as LR-M without rim APHE (Fig. 3). Except for the higher serum PIVKA-II level in the LR-M with rim APHE group and the higher ratio of women in the LR-M without rim APHE group, the other clinical factors did not differ significantly (Supplementary Table 2).

### MRI and Pathologic Features of HCC

MRI features: Supplementary Tables 2 and 3 summarize the MRI features of the HCCs. HCCs categorized as LR-4/5 (median size, 2.5 cm) were smaller than those categorized as either LR-M with rim APHE (median 3 cm,  $p = 0.031$ ) or LR-M without rim APHE (median 2.8 cm;  $p = 0.021$ ).

The three MVI imaging features (non-smooth tumor margin, peritumoral enhancement on AP, and peritumoral hypointensity on HBP) were more frequently observed in the LR-M with rim APHE group (84.0% [21/25], 36.0% [9/25], and 52.0% [13/25], respectively) than in the LR-4/5 group (47.9% [91/190], 16.3% [31/190], and 21.1% [40/190], respectively; all  $p < 0.05$ ). Interobserver agreement for

**Table 1. Baseline Characteristics of the Study Patients**

Variable	LR-4/5 (n = 190)	LR-M with Rim APHE (n = 25)	LR-M without Rim APHE (n = 27)	P
Age, years*	57.1 ± 9.8 (31–84)	55.2 ± 9.6 (37–74)	59.5 ± 9.9 (41–76)	0.295
Sex				0.018
Male	156 (82.1)	18 (72.0)	16 (59.3)	
Female	34 (17.9)	7 (28.0)	11 (40.7)	
Etiology of liver disease				0.968
Hepatitis B	155 (81.5)	22 (88.0)	22 (81.5)	
Hepatitis C	17 (9.0)	1 (4.0)	2 (7.4)	
Alcohol	1 (0.5)	0 (0)	0 (0)	
Others	17 (9.0)	2 (8.0)	3 (11.1)	
Liver cirrhosis	87 (45.8)	11 (44.0)	10 (37.0)	0.692
Child-Pugh grade				> 0.999
A	190 (100)	25 (100)	27 (100)	
ALBI grade				0.733
Grade 1	175 (92.1)	24 (96.0)	26 (96.3)	
Grade 2	15 (7.9)	1 (4.0)	1 (3.7)	
AFP, ng/mL <sup>†</sup>	13.9 (1.3–47524.4)	20.4 (1.3–3081.1)	10.9 (1.3–10569.6)	0.519
PIVKA-II, AU/mL <sup>†</sup>	32 (12–4231)	168 (13–35940)	33 (16–19176)	0.024
Tumor size, cm <sup>†</sup>	2.5 (0.9–4.8)	3.0 (1.5–4.7)	2.8 (1.9–4.7)	0.003

Except where indicated, data indicate the numbers of patients, with percentages in parentheses.  $p$  values were determined by comparing characteristics across the three LR categories. \*Data indicates means ± standard deviations, with ranges in parentheses, <sup>†</sup>Data indicate medians, with ranges in parentheses. AFP = alpha-fetoprotein, ALBI = albumin–bilirubin, APHE = arterial-phase hyperenhancement, PIVKA-II = protein induced by vitamin K absence or antagonist-II

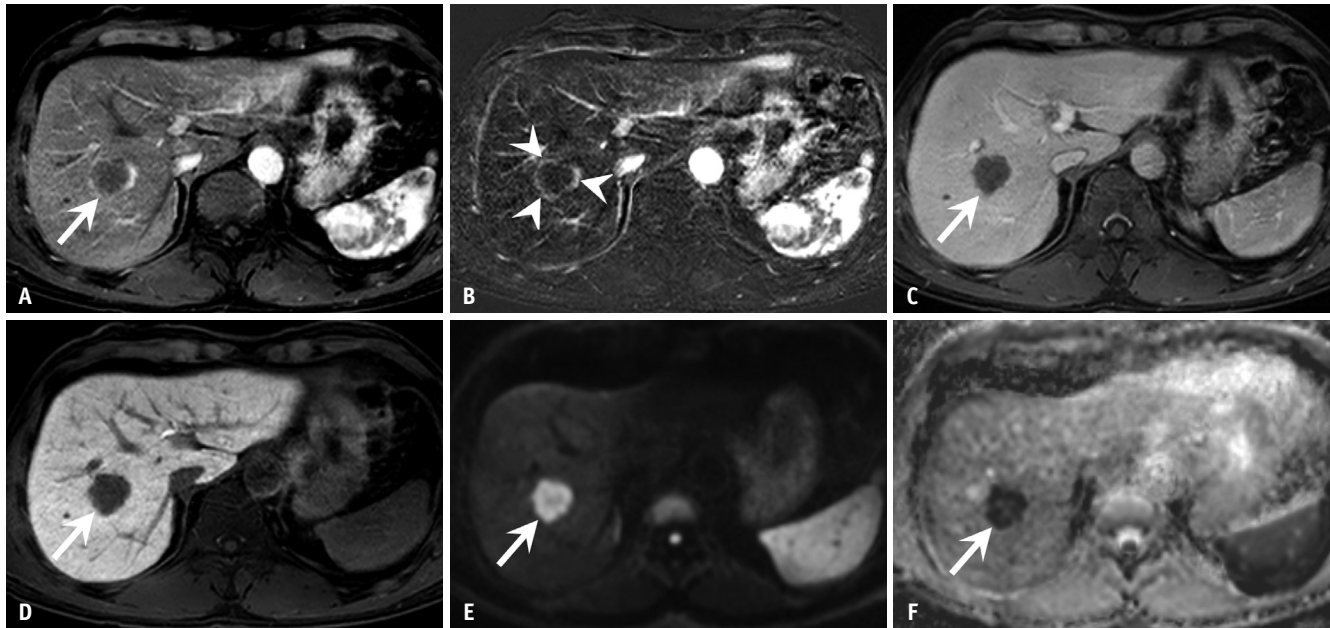


**Fig. 2. Hepatocellular carcinoma categorized as Liver Imaging Reporting and Data System category LR-M with rim APHE in a 55-year-old male.**

**A.** Gadoxetic acid-enhanced arterial-phase image shows a 2.8-cm-sized mass (arrow) with rim APHE in hepatic segment VIII. There was no peritumoral parenchymal enhancement on the arterial-phase images. **B.** The rim APHE (arrowheads) is obvious on the arterial subtraction image. **C.** Portal venous phase image shows a hypointense mass (arrow) compared to the surrounding liver parenchyma. **D.** Hepatobiliary phase images show hypointense mass (arrow). There was no peritumoral hypointensity. **E, F.** Diffusion-weighted image (**E**) and apparent diffusion coefficient map (**F**) showing the targetoid appearance (arrows). Multiple pulmonary metastases were noted 9.5 months after curative resection. APHE = arterial-phase hyperenhancement

the MRI features and the LI-RADS categories was good to excellent ( $\kappa = 0.71\text{--}0.87$ ). A detailed description of the interobserver agreements is provided in Supplementary Table 4.

**Pathologic features:** Histopathological examination revealed that the LR-M with rim APHE group tended to show poor tumor differentiation of HCCs (LR-4/5 vs. LR-M with rim APHE vs. LR-M without rim APHE; 8.4% [16/190] vs. 20.0% [5/25] vs. 3.7% [1/27],  $p = 0.095$ ) and more frequent MVI (35.8% [68/190] vs. 76.0% [19/25] vs. 59.3% [16/27],  $p < 0.001$ ) compared to those in the LR-4/5 group or the LR-M without rim APHE group (Table 2).

### Prognostic Factor Analysis

Table 3 summarizes the results of the univariable and multivariable analyses of the factors affecting OS and RFS. Multivariable analyses identified that the presence of liver cirrhosis (hazard ratio [HR] 5.16, 95% confidence interval [CI] 1.89–14.09;  $p = 0.001$ ), tumor size (HR 6.04, 95% CI 1.56–23.45;  $p = 0.009$ ), and LR-M with rim APHE (HR 5.48, 95% CI 1.72–17.50;  $p = 0.002$ ) were associated with OS. ALBI grade 2 (HR 2.15; 95% CI 1.05–4.42;  $p = 0.037$ ), tumor size (HR 1.77; 95% CI 1.13–2.79;  $p = 0.014$ ), and

LR-M with rim APHE (HR 2.09; 95% CI 1.02–4.27;  $p = 0.042$ ) were independent predictors of RFS.

### Survival Outcomes

The median follow-up period was 65 months (range, 7–83 months). At the time of analysis, 24 (9.9%) of the 242 patients had died (LR-4/5 vs. LR-M with rim APHE vs. LR-M without rim APHE, 7.4% [14/190] vs. 32.0% [8/25] vs. 7.4% [2/27],  $p < 0.002$ ). In addition, 81 (33.5%) of the 242 patients showed recurrence (33.2% [63/190] vs. 52.0% [13/25] vs. 18.5% [5/27],  $p = 0.037$ ).

OS and RFS differed according to LI-RADS category (Fig. 4). The 1-, 3-, and 5-year OS (92.0%, 76.0%, and 68.0%) and RFS (66.7%, 50.0%, and 45.8%) rates in the LR-M with rim APHE group were lower than those in the LR-4/5 group (OS: 99.5%, 97.3%, and 93.9%,  $p < 0.001$ ; RFS: 88.3%, 72.1%, and 66.8%,  $p = 0.047$  for RFS). However, the LR-M without rim APHE group (OS: 100%, 95.8%, and 91.3%  $p > 0.99$ ; RFS: 92.3%, 84.4%, and 80.2%,  $p = 0.448$ ) did not show significant differences in the 1-, 3-, and 5-year OS and RFS rates compared to those in the LR-4/5 group. There were no significant differences in OS rates between the LR-M with rim APHE and LR-M without rim APHE groups

( $p = 0.143$ ), whereas the RFS rates were worse in the LR-M with rim APHE group compared to those in the LR-M without rim APHE group ( $p = 0.022$ ).

## DISCUSSION

Our results suggest that the LI-RADS category on gadoxetic acid-enhanced MRI and tumor size were

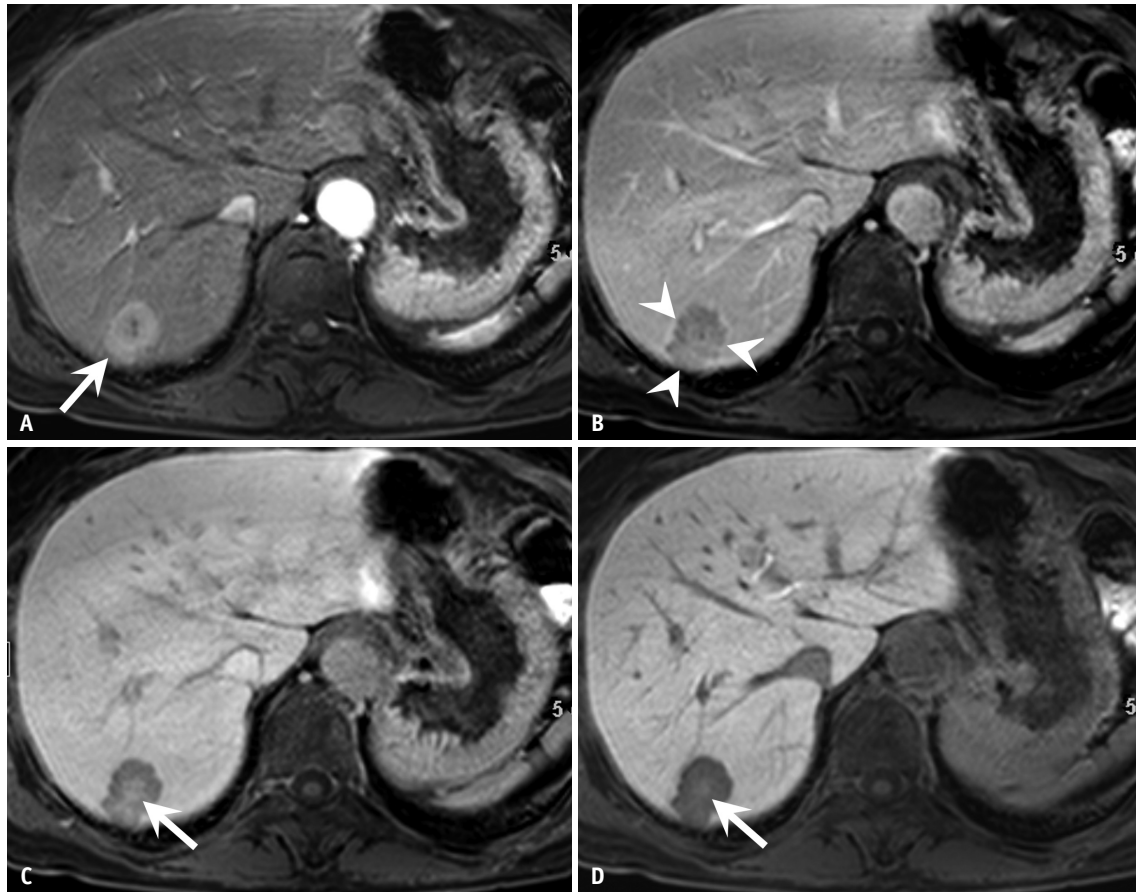


**Fig. 3.** Hepatocellular carcinoma categorized as Liver Imaging Reporting and Data System category LR-M without rim APHE in a 62-year-old female.

**A.** Gadoxetic acid-enhanced arterial-phase image shows a 2.9 cm-sized mass (arrow) with APHE in hepatic segment VII. There was no peritumoral parenchymal enhancement on the arterial-phase images. **B.** On the portal venous phase image, the mass shows washout. An enhancing capsule was noted (arrowheads). **C.** Transitional-phase image showing a mass with delayed central enhancement and a targetoid appearance (arrow). **D.** On the hepatobiliary phase image, the mass shows a targetoid appearance (arrow). Diffusion-weighted images show a hyperintense mass (not shown). Tumor recurrence was not noted during the 78.3-month follow-up period after curative resection. APHE = arterial-phase hyperenhancement

**Table 2.** Pathologic Features of HCCs according to LI-RADS Category

Variable	LR-4/5 (n = 190)	LR-M with Rim APHE (n = 25)	LR-M without Rim APHE (n = 27)	<i>P</i>
Differentiation				0.095
Grade I–II	174 (91.6)	20 (80.0)	26 (96.3)	
Grade III–IV	16 (8.4)	5 (20.0)	1 (3.7)	
MVI*				< 0.001
Yes	68 (35.8)	19 (76.0)	16 (59.3)	
No	122 (64.2)	6 (24.0)	11 (40.7)	

\*Two-sided adjusted *p* values for pairwise comparisons between the LI-RADS categories of HCCs were < 0.001 for LR-4/5 vs. LR-M with rim APHE, 0.033 for LR-4/5 vs. LR-M without rim APHE, and 0.322 for LR-M with rim APHE vs. LR-M without rim APHE. APHE = arterial-phase hyperenhancement, HCC = hepatocellular carcinoma, LI-RADS = Liver Imaging Reporting and Data System, MVI = microvascular invasion

**Table 3. Univariable and Multivariable Analyses of Factors Affecting Overall Survival and Recurrence-Free Survival**

Variables	Overall Survival			Recurrence-Free Survival		
	Univariable Analysis		Multivariable Analysis	Univariable Analysis		Multivariable Analysis
	HR (95% CI)	P	HR (95% CI)	HR (95% CI)	P	HR (95% CI)
Age, year*	1.04 (0.99, 1.08)	0.108		0.99 (0.95, 1.03)	0.652	
Female sex	1.54 (0.64, 3.71)	0.337		1.06 (0.63, 1.79)	0.830	
Liver cirrhosis	3.83 (1.52, 9.65)	0.004	5.16 (1.89, 14.09)	1.62 (1.05, 2.51)	0.030	1.55 (0.96, 2.50)
ALBI						
Grade 1	Reference			Reference		
Grade 2	1.37 (0.32, 5.82)	0.671		3.00 (1.54, 5.84)	0.001	2.15 (1.05, 4.42)
AFP, log ng/mL*	1.33 (0.94, 1.88)	0.108		1.20 (0.98, 1.46)	0.080	1.17 (0.95, 1.44)
PIVKA-II, log mAU/mL*	4.30 (1.66, 11.18)	0.003	1.12 (0.35, 3.59)	2.16 (1.27, 3.70)	0.005	1.42 (0.74, 2.75)
Tumor size, cm	9.14 (2.78, 30.07)	< 0.001	6.04 (1.56, 23.45)	2.16 (1.46, 3.20)	< 0.001	1.77 (1.13, 2.79)
LI-RADS category <sup>†</sup>						
LR-4/5	Reference			Reference		
LR-M with rim APHE	5.54 (2.03, 15.14)	< 0.001	5.48 (1.72, 17.50)	2.06 (1.04, 4.09)	0.035	2.09 (1.02, 4.27)
LR-M without rim APHE	1.13 (0.21, 6.15)	> 0.999	1.30 (0.23, 7.40)	0.52 (0.18, 1.47)	0.316	0.49 (0.17, 1.44)
Non-smooth tumor margin	6.86 (0.84, 55.93)	0.072	1.66 (0.17, 16.68)	1.30 (0.84, 2.02)	0.242	
Peritumoral parenchymal enhancement on AP	1.46 (0.58, 3.69)	0.419		1.41 (0.84, 2.35)	0.194	
Peritumoral hypointensity on HBP	1.83 (0.80, 4.19)	0.151		1.13 (0.69, 1.85)	0.623	

\* Log transformation was used for analysis of the preoperative AFP and PIVKA level, <sup>†</sup>LI-RADS categories were defined as LR-4 (probably HCC), LR-5 (definitely HCC), and LR-M (probably malignant, not specific for HCC). HR > 1 indicates increased risk of event (recur or death). AFP = alpha-fetoprotein, ALBI = albumin-bilirubin, AP = arterial phase, APHE = arterial-phase hyperenhancement, CI = confidence interval, HBP = hepatobiliary phase, HR = hazard ratio, LI-RADS = Liver Imaging Reporting and Data System, PIVKA-II = protein induced by vitamin K absence or antagonist-II

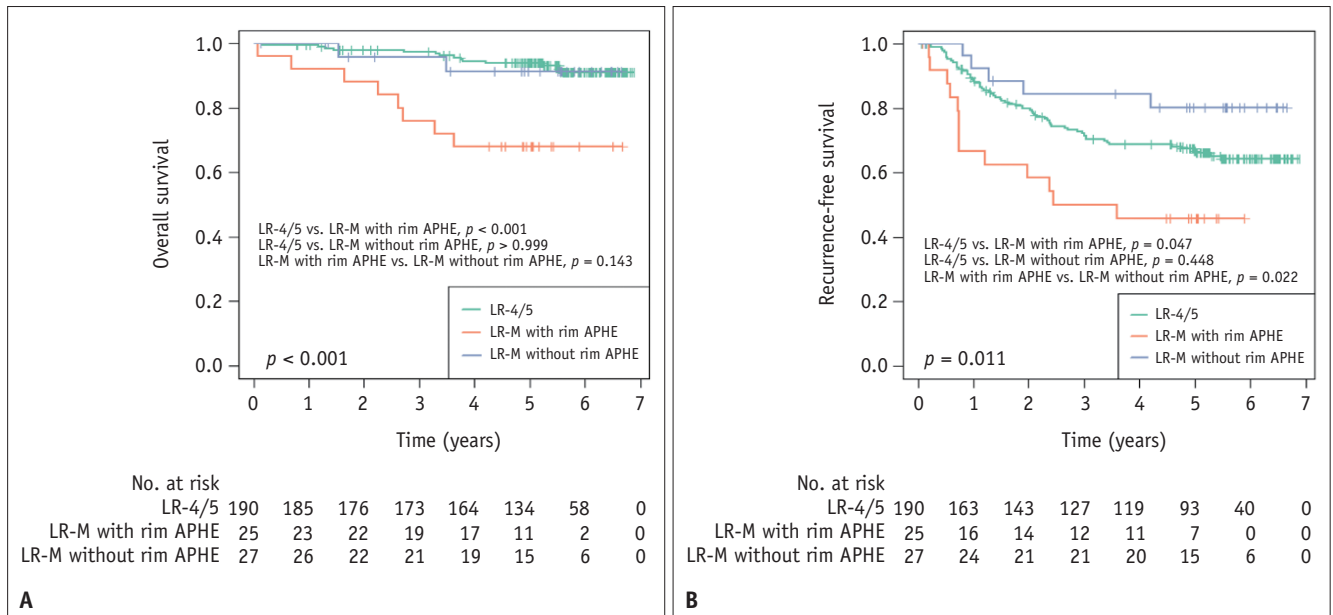


**Fig. 4. Survival analysis in 242 patients according to Liver Imaging Reporting and Data System category.**

**A.** Overall survival. **B.** Recurrence-free survival. APHE = arterial-phase hyperenhancement

significant factors associated with OS and RFS after resection of a single HCC ( $\leq 5$  cm) in patients with chronic liver disease. In our study, HCCs categorized as LR-M due to rim APHE had the worst prognosis after surgical resection. The postoperative prognosis of HCC classified as LR-M because of other targetoid features (especially TP or HBP targetoid appearance) without rim APHE did not differ from that of HCCs classified as LR-4/5. Thus, rim APHE may predict the postoperative prognosis of HCC after further stratification of LR-M on preoperative MRI. The three known MVI imaging features (non-smooth tumor margin, peritumoral enhancement on AP image, and peritumoral hypointensity on HBP image) were not significantly associated with OS and RFS.

A notable aspect of our study was that among the targetoid features, rim APHE was a more reliable predictor of worse prognosis than the other targetoid appearances. This finding may be attributable to the higher proportion of HCCs with poor tumor differentiation (20.0% [5/25]) and the more frequent MVI (76.0% [19/25]) in the LR-M with rim APHE group than in the LR-4/5 (8.4% [16/190] and 35.8% [68/190], respectively) and LR-M without rim APHE (3.7% [1/27] and 59.3% [16/27], respectively) groups. Most studies have consistently found that rim APHE of HCC is related to poor tumor grade, MVI, or cytokeratin 19-positive HCC; hence, it is related to worse prognosis [13,14,28,29]. Our results are similar to those of Rhee et

al. [14], who reported aggressive histopathologic features of HCCs with rim APHE compared to HCCs without rim APHE. Thus, rim APHE may be a more reliable imaging biomarker for aggressive HCC than other targetoid features.

In addition, our results were consistent with those of previous reports showing the usefulness of LI-RADS category as a prognostic imaging biomarker for primary liver carcinomas, including HCCs, intrahepatic cholangiocarcinomas, and combined hepatocellular-cholangiocarcinomas [17,18]. Unlike previous studies, however, we focused on the capability of each targetoid feature of the LR-M category to enable further stratification of HCC prognosis. Furthermore, we evaluated the pathological mechanism of the prognostic value of the LI-RADS category.

MVI, which is histopathologically diagnosed only after surgical resection, is a well-known independent prognostic factor in patients with HCC after resection or liver transplantation [9,30]. In our study, the known imaging features predictive of MVI were not associated with postoperative prognosis, contrary to a previous report [21]. Lee et al. [21] reported that the presence of two or more of the three MVI imaging features could serve as a preoperative imaging biomarker for predicting MVI with a specificity  $> 90\%$  and that this finding was associated with early recurrence after curative resection of a single HCC. This difference may be due to the different primary outcomes (presence



of early recurrence vs. OS and RFS not limited to the early postoperative period in our study) and the combination of significant findings or whether each was used independently. Therefore, our results require further validation in prospective studies with larger numbers of patients.

Our study evaluated both LI-RADS category and MVI imaging features not incorporated in the LI-RADS in terms of postoperative prognosis. Our results suggested that further stratification using LI-RADS categories based on rim APHE could be a more relevant prognostic imaging biomarker than each MVI feature alone. Thus, the LI-RADS category might provide more comprehensive information using known imaging features that are related to the pathological characteristics of HCCs compared to individual MVI imaging features.

Our results also showed that tumor size was a significant predictor of postoperative prognosis. These findings agree with those of previous studies in which large tumor size was associated with more frequent vascular invasion, advanced histologic grade, intrahepatic metastasis, and early tumor recurrence [10,12,31,32]. In a large study of 57920 HCC patients, Wu et al. [33] reported that tumor size at diagnosis was an independent prognostic factor for the survival of patients with HCC.

The ALBI grade has been validated as a prognostic factor for OS in HCC [34]. Several studies have also reported that the ALBI grade is a feasible predictive marker for tumor recurrence in post-resection HCC [35,36]. Consistent with previous studies, ALBI grade 2 was an independent predictor of RFS in our study. We speculate that impaired liver function may be associated with early HCC recurrence.

Our study had several limitations. First, we included only surgically resected single HCCs, possibly creating a selection bias and precluding generalization to patients with multiple HCCs. Second, there is a potential risk of selection bias because we excluded patients with less than 6 months of follow-up. This may have resulted in the exclusion of patients with early postoperative deaths. Third, our study population mostly consisted of Child-Pugh class A cases, preventing the generalization of the study findings to cases with advanced liver cirrhosis. Fourth, we did not include non-HCC primary liver cancers because we focused on the postsurgical prognosis of HCC. Finally, the cases were obtained from a single center in an area endemic for hepatitis B virus infection. Therefore, a prospective, confirmatory follow-up study should include stratification of liver function and validation of patients with disease

etiology from multiple centers.

In conclusion, further classification of the LR-M category by imaging according to the presence of rim APHE may help to noninvasively predict the postoperative prognosis of patients with a single HCC.

## Supplement

The Supplement is available with this article at <https://doi.org/10.3348/kjr.2020.1428>.

## Conflicts of Interest

The authors have no potential conflicts of interest to disclose.

## Author Contributions

Conceptualization: Ji Yoon Moon, Ji Hye Min, Young Kon Kim. Data curation: Ji Yoon Moon, Ji Hye Min. Formal analysis: Seon Woo Kim, Ho-Jeong Won. Investigation: Ji Yoon Moon, Donglk Cha, Jeong Ah Hwang. Methodology: Ji Hye Min, Seo-Youn Choi. Project administration: Ji Hye Min. Supervision: Young Kon Kim. Validation: Seong Eun Ko, Eun Joo Yun. Visualization: Ji Yoon Moon, Ji Hye Min. Writing—original draft: Ji Yoon Moon, Ji Hye Min. Writing—review & editing: all authors.

## ORCID iDs

Ji Yoon Moon

<https://orcid.org/0000-0003-3758-2617>

Ji Hye Min

<https://orcid.org/0000-0002-8496-6771>

Young Kon Kim

<https://orcid.org/0000-0002-6854-400X>

Donglk Cha

<https://orcid.org/0000-0003-3271-6532>

Jeong Ah Hwang

<https://orcid.org/0000-0002-8012-995X>

Seong Eun Ko

<https://orcid.org/0000-0003-0007-6569>

Seo-Youn Choi

<https://orcid.org/0000-0002-2434-8779>

Eun Joo Yun

<https://orcid.org/0000-0001-9310-4340>

Seon Woo Kim

<https://orcid.org/0000-0002-9236-560X>

Ho-Jeong Won

<https://orcid.org/0000-0002-8590-1654>

## REFERENCES

- Liu PH, Hsu CY, Hsia CY, Lee YH, Huang YH, Chiou YY, et al. Surgical resection versus radiofrequency ablation for single hepatocellular carcinoma  $\leq 2$  cm in a propensity score model. *Ann Surg* 2016;263:538-545
- Takayama T, Makuuchi M, Hasegawa K. Single HCC smaller than 2 cm: surgery or ablation?: surgeon's perspective. *J Hepatobiliary Pancreat Sci* 2010;17:422-424
- Forner A, Reig M, Bruix J. Hepatocellular carcinoma. *Lancet* 2018;391:1301-1314
- Bruix J, Gores GJ, Mazzaferro V. Hepatocellular carcinoma: clinical frontiers and perspectives. *Gut* 2014;63:844-855
- Feng J, Chen J, Zhu R, Yu L, Zhang Y, Feng D, et al. Prediction of early recurrence of hepatocellular carcinoma within the Milan criteria after radical resection. *Oncotarget* 2017;8:63299-63310
- Chen J, Zhou J, Kuang S, Zhang Y, Xie S, He B, et al. Liver imaging reporting and data system category 5: MRI predictors of microvascular invasion and recurrence after hepatectomy for hepatocellular carcinoma. *AJR Am J Roentgenol* 2019;213:821-830
- Chan AWH, Zhong J, Berhane S, Toyoda H, Cucchetti A, Shi K, et al. Development of pre and post-operative models to predict early recurrence of hepatocellular carcinoma after surgical resection. *J Hepatol* 2018;69:1284-1293
- Braunwarth E, Stättner S, Fodor M, Cardini B, Resch T, Oberhuber R, et al. Surgical techniques and strategies for the treatment of primary liver tumours: hepatocellular and cholangiocellular carcinoma. *Eur Surg* 2018;50:100-112
- Agopian VG, Harlander-Locke M, Zarrinpar A, Kaldas FM, Farmer DG, Yersiz H, et al. A novel prognostic nomogram accurately predicts hepatocellular carcinoma recurrence after liver transplantation: analysis of 865 consecutive liver transplant recipients. *J Am Coll Surg* 2015;220:416-427
- An C, Kim DW, Park YN, Chung YE, Rhee H, Kim MJ. Single hepatocellular carcinoma: preoperative MR imaging to predict early recurrence after curative resection. *Radiology* 2015;276:433-443
- Lee S, Kim KW, Jeong WK, Kim MJ, Choi GH, Choi JS, et al. Gadoteric acid-enhanced MRI as a predictor of recurrence of HCC after liver transplantation. *Eur Radiol* 2020;30:987-995
- Pawlik TM, Delman KA, Vauthey JN, Nagorney DM, Ng IO, Ikai I, et al. Tumor size predicts vascular invasion and histologic grade: implications for selection of surgical treatment for hepatocellular carcinoma. *Liver Transpl* 2005;11:1086-1092
- Choi SY, Kim SH, Park CK, Min JH, Lee JE, Choi YH, et al. Imaging features of gadoteric acid-enhanced and diffusion-weighted MR imaging for identifying cytokeratin 19-positive hepatocellular carcinoma: a retrospective observational study. *Radiology* 2018;286:897-908
- Rhee H, An C, Kim HY, Yoo JE, Park YN, Kim MJ. Hepatocellular carcinoma with irregular rim-like arterial phase hyperenhancement: more aggressive pathologic features. *Liver Cancer* 2019;8:24-40
- American College of Radiology. CT/MRI LI-RADS® v2018. Acr.org Web site. <https://www.acr.org/Clinical-Resources/Reporting-and-Data-Systems/LI-RADS/CT-MRI-LI-RADS-v2018>. Accessed August 15, 2019
- Jeon SK, Joo I, Lee DH, Lee SM, Kang HJ, Lee KB, et al. Combined hepatocellular cholangiocarcinoma: LI-RADS v2017 categorisation for differential diagnosis and prognostication on gadoteric acid-enhanced MR imaging. *Eur Radiol* 2019;29:373-382
- Choi SH, Lee SS, Park SH, Kim KM, Yu E, Park Y, et al. LI-RADS classification and prognosis of primary liver cancers at gadoteric acid-enhanced MRI. *Radiology* 2019;290:388-397
- An C, Park S, Chung YE, Kim DY, Kim SS, Kim MJ, et al. Curative resection of single primary hepatic malignancy: liver imaging reporting and data system category LR-M portends a worse prognosis. *AJR Am J Roentgenol* 2017;209:576-583
- Kierans AS, Leonardou P, Hayashi P, Brubaker LM, Elazzazi M, Shaikh F, et al. MRI findings of rapidly progressive hepatocellular carcinoma. *Magn Reson Imaging* 2010;28:790-796
- Bruix J, Reig M, Sherman M. Evidence-based diagnosis, staging, and treatment of patients with hepatocellular carcinoma. *Gastroenterology* 2016;150:835-853
- Lee S, Kim SH, Lee JE, Sinn DH, Park CK. Preoperative gadoteric acid-enhanced MRI for predicting microvascular invasion in patients with single hepatocellular carcinoma. *J Hepatol* 2017;67:526-534
- Reginelli A, Vacca G, Segreto T, Picascia R, Clemente A, Urraro F, et al. Can microvascular invasion in hepatocellular carcinoma be predicted by diagnostic imaging? A critical review. *Future Oncol* 2018;14:2985-2994
- Ariizumi S, Kitagawa K, Kotera Y, Takahashi Y, Katagiri S, Kuwatsuru R, et al. A non-smooth tumor margin in the hepatobiliary phase of gadoteric acid disodium (Gd-E0B-DTPA)-enhanced magnetic resonance imaging predicts microscopic portal vein invasion, intrahepatic metastasis, and early recurrence after hepatectomy in patients with hepatocellular carcinoma. *J Hepatobiliary Pancreat Sci* 2011;18:575-585
- Kim H, Park MS, Choi JY, Park YN, Kim MJ, Kim KS, et al. Can microvessel invasion of hepatocellular carcinoma be predicted by pre-operative MRI? *Eur Radiol* 2009;19:1744-1751
- Cha DI, Jang KM, Kim SH, Kim YK, Kim H, Ahn SH. Preoperative prediction for early recurrence can be as accurate as postoperative assessment in single hepatocellular carcinoma patients. *Korean J Radiol* 2020;21:402-412
- Kim KA, Kim MJ, Jeon HM, Kim KS, Choi JS, Ahn SH, et al. Prediction of microvascular invasion of hepatocellular carcinoma: usefulness of peritumoral hypointensity seen on gadoteric acid disodium-enhanced hepatobiliary phase images. *J Magn Reson Imaging* 2012;35:629-634
- Rodríguez-Perálvarez M, Luong TV, Andreana L, Meyer T, Dhillon AP, Burroughs AK. A systematic review of

- microvascular invasion in hepatocellular carcinoma: diagnostic and prognostic variability. *Ann Surg Oncol* 2013;20:325-339
28. Jeong HT, Kim MJ, Kim YE, Park YN, Choi GH, Choi JS. MRI features of hepatocellular carcinoma expressing progenitor cell markers. *Liver Int* 2012;32:430-440
29. Roayaie S, Obeidat K, Sposito C, Mariani L, Bhoori S, Pellegrinelli A, et al. Resection of hepatocellular cancer  $\leq 2$  cm: results from two Western centers. *Hepatology* 2013;57:1426-1435
30. Roayaie S, Blume IN, Thung SN, Guido M, Fiel MI, Hiotis S, et al. A system of classifying microvascular invasion to predict outcome after resection in patients with hepatocellular carcinoma. *Gastroenterology* 2009;137:850-855
31. Renzulli M, Brocchi S, Cucchetti A, Mazzotti F, Mosconi C, Sportoletti C, et al. Can current preoperative imaging be used to detect microvascular invasion of hepatocellular carcinoma? *Radiology* 2016;279:432-442
32. Taketomi A, Sanefuji K, Soejima Y, Yoshizumi T, Uchiyama H, Ikegami T, et al. Impact of des-gamma-carboxy prothrombin and tumor size on the recurrence of hepatocellular carcinoma after living donor liver transplantation. *Transplantation* 2009;87:531-537
33. Wu G, Wu J, Wang B, Zhu X, Shi X, Ding Y. Importance of tumor size at diagnosis as a prognostic factor for hepatocellular carcinoma survival: a population-based study. *Cancer Manag Res* 2018;10:4401-4410
34. Toyoda H, Lai PB, O'Beirne J, Chong CC, Berhane S, Reeves H, et al. Long-term impact of liver function on curative therapy for hepatocellular carcinoma: application of the ALBI grade. *Br J Cancer* 2016;114:744-750
35. Ho SY, Hsu CY, Liu PH, Hsia CY, Su CW, Huang YH, et al. Albumin-bilirubin (ALBI) grade-based nomogram to predict tumor recurrence in patients with hepatocellular carcinoma. *Eur J Surg Oncol* 2019;45:776-781
36. Lee YH, Koh YS, Hur YH, Cho CK, Kim HJ, Park EK. Effectiveness of the albumin-bilirubin score as a prognostic factor for early recurrence after curative hepatic resection for hepatocellular carcinoma. *Ann Hepatobiliary Pancreat Surg* 2018;22:335-343